A Simple Method to Build a Paper-Based Color Check Print of Colored Fabrics by Conventional Printers

Sajjad Fashandi sfashandi@aut.ac.ir
MSc./Department of Textile Engineering
Amirkabir University of Technology (Tehran Polytechnic)
Tehran, 15914, Iran

Seyed Hossein Amirshahi hamirsha@aut.ac.ir
Professor/Department of Textile Engineering
Amirkabir University of Technology (Tehran Polytechnic)
Tehran, 15914, Iran

Shahram Peyvandi peyvandi@aut.ac.ir
PhD/Department of Textile Engineering
Amirkabir University of Technology (Tehran Polytechnic)
Tehran, 15914, Iran

Abstract

An open loop color management system is implemented to reproduce an analog color of a set of colored fabrics by a digital inkjet printer. A tetrahedral interpolation technique is designed for mapping between device-dependent (RGB) and device-independent (CIELAB) color spaces. A set of 3164 color patches are used as training set in 3-D LookUp Table (LUT) to characterize the color printer. Then, the designed color management system is examined by the colorimetric reproduction of a set of 30 colored fabrics using the conventional inkjet printer. The performance of the system is numerically evaluated by measuring the color difference values between the original and the reproduced samples. The results showed that the color reproduction system appropriately works for both groups of samples located inside the color gamut of output device, i.e. printer, and those out of gamut samples while the later logically leads to greater errors.

Keywords: Color Management System (CMS), Inkjet Color Printer, Colorimetric Reproduction, Lookup Table (LUT), Paper Check Print.

1. INTRODUCTION

The most applicable color matching algorithms in the traditional analog color reproduction, in which the colorant concentrations and the corresponding tristimulus values continuously change, were developed by Allen based on the single and two constant Kubelka-Munk theories [1, 2]. While the suggested methodologies try to match the colorimetric tristimulus values of target under a given set of viewing conditions, some methods based on the least squares fitting of reflectance spectrum of target was developed and is known as spectrophotometric matching [3].

In the recent decades, the modern digital instruments have been developed for color reproduction of scenes and objects. The more advanced color reproduction devices with digitally adjustable user controls have become more popular in the past few years and widely used in different media such as paper, plastic, textile as well as displaying units [4]. The simplicity of producing colors in the digital instruments especially in the forms of printed papers and display units has led to introducing some systems for successful transformation of colors within different digital devices like scanners, cameras, printers and monitors. The accurate reproduction of colors between different digital instruments would be guaranteed by an appropriate color management system (CMS). By using the CMS, all input digital signals (mostly in RGB color space) are mapped into a standard color space (CIEXYZ or CIELAB) and finally digital signals (RGB or CMYK) are delivered in output devices. The intermediate analog color space is called as profile connection space (PCS) and known as the "heart of CMS" [5, 6].

A type of conversion between the analog and digital colors occurs in digital devices such as monitors and printers. Several methods, such as polynomial transforms [7], physical models [8-10], artificial neural networks (ANNs) [11] and lookup tables (LUTs) [12] have been proposed to establish such mutual connections. Zhang *et al.* [7] employed the polynomial transforms for mapping XYZ tristimulus values of color patches to those of CMYK signals. They used IT 8.7/2-1993 color chart with 286 patches to specify the coefficients of polynomial transforms. Eq. 1 simply shows the first order polynomial transformation in matrix form, in which the tristimulus values *XYZ* are predicted from *CMYK* signals. Results of utilizing the second, third and fourth order polynomial transformations were also reported in mentioned article.

$$\begin{bmatrix} X \\ Y \\ Z \end{bmatrix} = \begin{bmatrix} a_1 & a_2 & a_3 & a_4 & a_5 \\ a_6 & a_7 & a_8 & a_9 & a_{10} \\ a_{11} & a_{12} & a_{13} & a_{14} & a_{15} \end{bmatrix} \begin{bmatrix} C \\ M \\ Y \\ K \\ 1 \end{bmatrix} \quad (1)$$

Bezerra *et al.* [8] used partitive color mixing theory as a physical model to predict the colors on paper using a paper ink-jet printer. The mathematical approach of the model is shown by Eq. 2,

$$\begin{aligned} X_{mix} &= \sum_i a_i X_i \\ Y_{mix} &= \sum_i a_i Y_i \\ Z_{mix} &= \sum_i a_i Z_i \end{aligned} \quad (2)$$

where, X_{mix}, Y_{mix}, Z_{mix} and X_i, Y_i, and Z_i are the tristimulus values of the mixture and the i[th] colors, respectively and a_i are the fractional areas of the colors, i.e., $\sum_i a_i = 1$. As shown by Eq. 3, the resultant color $(X_{mix}, Y_{mix}, Z_{mix})$ of the overall image could be then calculated by the Neugebauer equations and the summation of the weighted tristimulus values of all fractional areas that could be eight for a CMY printer.

$$\begin{aligned} X_{mix} &= (1-c)(1-m)(1-y)X_W + c(1-m)(1-y)X_C + m(1-c)(1-y)X_M + y(1-m)(1-c)X_Y + my(1-c)X_R + \\ &\quad cy(1-m)X_G + cm(1-y)X_B + cmyX_K . \\ Y_{mix} &= (1-c)(1-m)(1-y)Y_W + c(1-m)(1-y)Y_C + m(1-c)(1-y)Y_M + y(1-m)(1-c)Y_Y + my(1-c)Y_R + \\ &\quad cy(1-m)Y_G + cm(1-y)Y_B + cmyY_K . \\ Z_{mix} &= (1-c)(1-m)(1-y)Z_W + c(1-m)(1-y)Z_C + m(1-c)(1-y)Z_M + y(1-m)(1-c)Z_Y + my(1-c)Z_R + \\ &\quad cy(1-m)Z_G + cm(1-y)Z_B + cmyZ_K . \end{aligned} \quad (3)$$

in which, the subscripts C, M, Y, R, G, B, W and K respectively stand for cyan, magenta, yellow, red, green, blue, white and black to represent the corresponding *X*, *Y* and *Z* tristimulus values. The areas covered by such subtractive primaries cyan, magenta, yellow are shown by *c*, *m* and *y*, respectively.

Zuffi *et al.* [9] employed a physical model to spectrally characterize the printers. They used the Yule-Nielsen spectral Neugebauer equation to model the printer. The authors also used the genetic algorithm to estimate the model's parameters. The genetic algorithm was also employed to tune a spectral printer model based on the Yule-Nielsen modified Neugebauer equation [10]. Three different types of printers as well as different papers and printer drivers were used in this research. An artificial neural networks (ANN) was used by Vrhel [11] to approximate the color characterization of multilayer lookup table (MLUT). While the MLUT could be logically large for such embedded systems, the ANN was used to provide a more compressed version of function approximation. Vrhel *et al.* [12] used the MLUT technique to map the device-dependent color space (RGB values) to the device-independent standard CIELAB color space ($L^* a^* b^*$ values).

In the present paper, a standard 3D-LUT and a tetrahedral interpolation technique are used to map the device-independent color space (CIELAB) of colored fabrics to device-dependent color space (RGB). In fact, the CIE $L^* a^* b^*$ colorimetric values of colored fabrics are converted to an RGB color space and reproduced by a commercial printer on paper. Whereas some input colors are not in the gamut of destination space that is the color inkjet printer, they are clipped into the gamut of the printer by a centroid clipping color gamut mapping algorithm. Since the color reproduction of textile through a coloration process requires a time and energy consuming procedure, the main goal of the present research is to reproduce the colors of textiles on paper using an inkjet printer for presenting a color check print with known CIELAB values.

2. DESIGNING A TYPICAL CMS

To set up a typical color management system (CMS), some principles for printer mapping, inverse printer mapping and the gamut mapping were employed in this research.

2.1. Printer Map

For mapping between the RGB and the CIELAB values, a tetrahedral interpolation technique was used [13]. The technique is a precise method for interpolating the regularly sampled LUTs. As Figure 1 shows, the tetrahedral interpolation technique divides a cube into six tetrahedrons. The interpolated values are the weighted sum of the values of the function at the four vertices of the tetrahedral enclosing the desired points. The formulation of the method could be described by Eq. 4,

$$P = P_{000} + P_x \frac{x - x_0}{x_1 - x_0} + P_y \frac{y - y_0}{y_1 - y_0} + P_z \frac{z - z_0}{z_1 - z_0} \tag{4}$$

where, the surrounding eight nodes in the RGB color space are [n_{000} n_{001} n_{010} n_{011} n_{100} n_{101} n_{110} n_{111}] and the corresponding points in the CIELAB space are [p_{000} p_{001} p_{010} p_{011} p_{100} p_{101} p_{110} p_{111}], while the $[x_0\ y_0\ z_0]$ and $[x_1\ y_1\ z_1]$ are the coordinates of n_{000} and n_{111} respectively. The expressions for P_x, P_y and P_z depend on the location of P with respect to the six tetrahedrons and as the result, the output P could be found through the proposed $[x\ y\ z]$ input values.

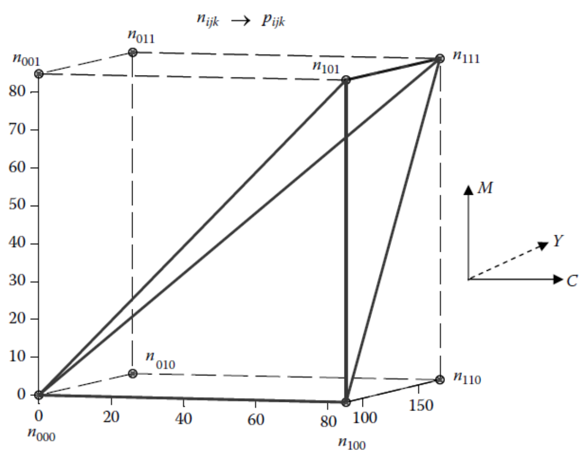

FIGURE 1: The Tetrahedral Interpolation [14].

The printer inverse model could be theoretically viewed as an inverse LUT and simply could be achieved from the inverse of the forward LUT; however, the method is not practically applicable. In fact, this kind of LUT may not be well defined for the colors at the boundary of gamut and may lead to multivalued outputs [14].

2.2. Inverse Printer Map

Multidimensional interpolation approaches, such as tetrahedral, conjugate gradient (CG) and iteratively clustered interpolation (ICI) algorithms are often used to produce inverse printer map [14]. In this research, the ICI algorithm is used to invert the forward model of printer. The algorithm is a gradient-based optimization method that improves the initial points by using an iterative technique [15].

2.3. The Printer Color Gamut Mapping

The printer gamut is usually restricted to a significantly smaller range in comparison to the gamut of the source digital image due to the physical limitations of the printer's primaries. The colors that could be found in the source gamut and would not be available in the output gamut are said to be out of gamut and should be converted to printable colors through a transformation technique called gamut mapping. Different techniques such as gamut clipping and gamut compression were suggested to deal with such problem [14]. In this paper, the centroid clipping color gamut mapping algorithm was used to map the out of gamut colors into the printer gamut [16].

3. EXPERIMENTAL

Three essential algorithms, i.e. tetrahedral interpolation for printer mapping, inverse printer map and color gamut mapping were designed in this research to perform the experimental study. Unlike the typical color management systems in which PCS is an intermediate analog color space, the PCS was considered as the initial space for input in the designed CMS in this research. Actually, the major difference between the employed and the classical CMSs is the profile connection space that opposed to classical method, it uses the analogue L*a*b* colorimetric data as inputs and provides digital RGB values in the outputs. In fact, the model could be considered as an abridged version of the general CMS model. In the other words, instead of using a digital image as input, analog tristimulus values of a colored fabric are used as inputs of designed CMS. In fact, the designed CMS could be considered as a digital approach for color matching in textile industry.

3.1. Training Color Charts

In this research, the training color charts were produced with Adobe Illustrator CS5. The color management system was turned off in this software to produce color charts. A tonal range of a unique hue was considered to create 126 color patches on each page. Subsequently, the saturation and lightness of colors of a given hue respectively varied from left to right and top to bottom for each hue. Accordingly, with 25 different hues on each page and 14 gray samples (gray ramp), the total of 3164 color patches were prepared to characterize the printer.

In order to achieve digital images from vector-base objects that were designed in Adobe Illustrator CS5, the produced colored samples were exported to Adobe Photoshop CS5. The color management system of software was again deactivated to avoid any possible change in the original values of color specifications. A low price commercial CMYK color printer named Epson Stylus T27 was used as the printing device. The color charts were printed on 260 $g\,m^{-2}$ A4 quality photo glossy papers that is commercially named EUNP5080 and supplied by UNIK Int. In fact, the small dot gain and good reproducibility can be expected by this type of paper. The original inks from Epson were used in printing process whose spectral reflectances are presented in Figure 2. The reflectance spectra of printed samples were measured from 400 nm to 700 nm at 10 nm intervals using a portable spectrophotometer named Eye One Pro from GretagMacbeth. Figure 3 shows the CIE a^*b^* and L^*C^* scatter-plots of the printer inks under D65 illuminant and 1964 standard observer.

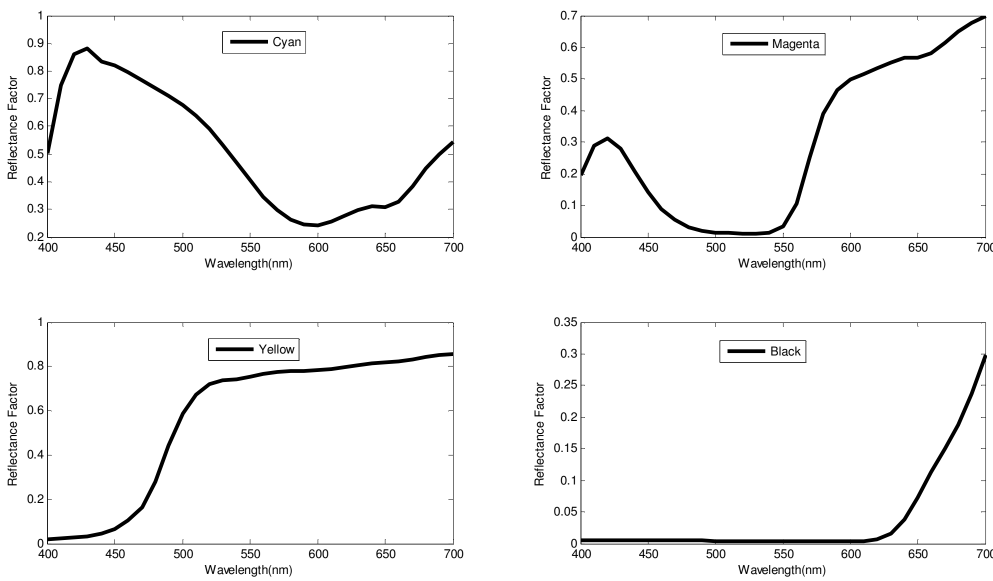

FIGURE 2: The Reflectance Spectra of Printer Primaries.

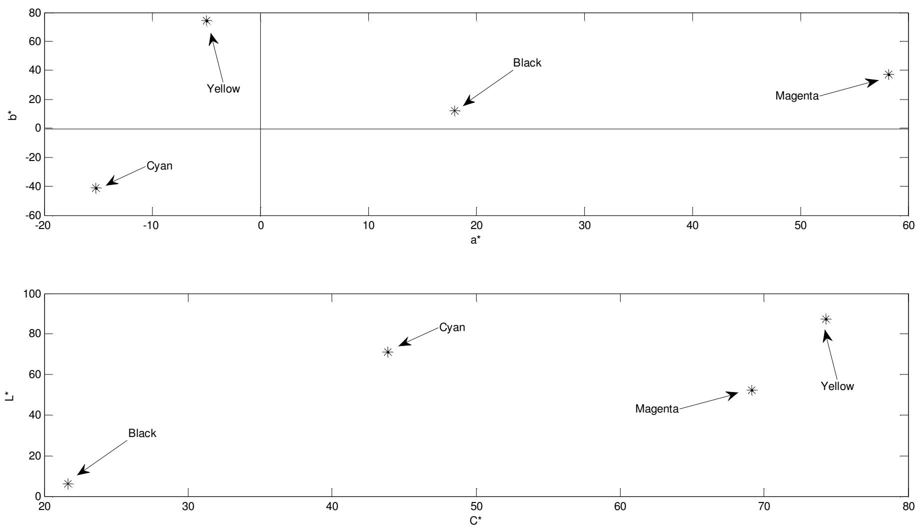

FIGURE 3: The CIE *a*b** and *C*L** Plots of Printer Primaries.

Since the Epson Stylus T27 is not a postscript printer, the RGB values were used as device dependent color space [17]. The produced color charts were firstly converted to TIFF format, with no embedded ICC profile in the Adobe Photoshop CS5, to determine the RGB values of color patches for further computations. It should be emphasized that the RGB values in TIFF format are as same as PSD format and the Adobe Photoshop CS5 was only an intermediate platform for producing and printing of training charts. Figure 4 shows the block diagram of the training charts production, printing and measuring attempts that were made in this work.

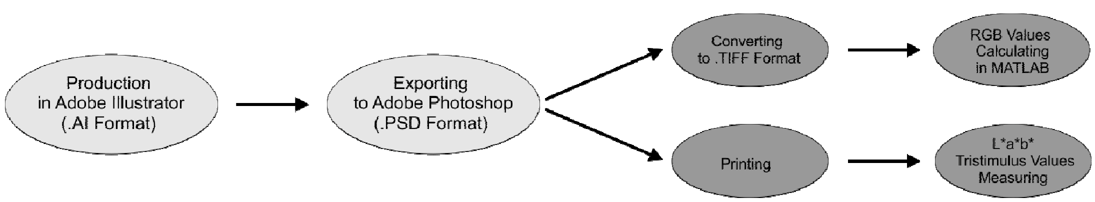

FIGURE 4: The block diagram of production of training charts, printing and color measuring attempts.

3.2. Test Color Chart

In order to evaluate the performance of the designed color management system and the efficacy of printer characterization, the spectral reflectances of 30 colored fabrics were measured using the GretagMacbeth Color-Eye 7000A spectrophotometer. The spectrophotometer benefited from integrated sphere with d/8 measurement geometry that makes it suitable for measuring the reflectance spectra of textured surfaces such as textiles. The spectral range was from 400 nm to 700 nm at 10 nm intervals. The specular component of reflectance was excluded and the medium aperture was used. Similar to the training charts, the CIELAB color values of samples were computed under D65 illuminant and 1964 standard observer. The CIE a^*b^* and L^*C^* scatter plots of colored fabrics are shown in Figure 5. The colorimetric values of the colored fabrics were considered as the target color for reproduction on paper media. To do so, the computed colorimetric values were imported as input data to the designed color management system and the resultant images were exported in TIFF format as output. Same as training color charts, Adobe Photoshop CS5, was employed to print the images. Figure 6 shows the block diagram of the designed CMS.

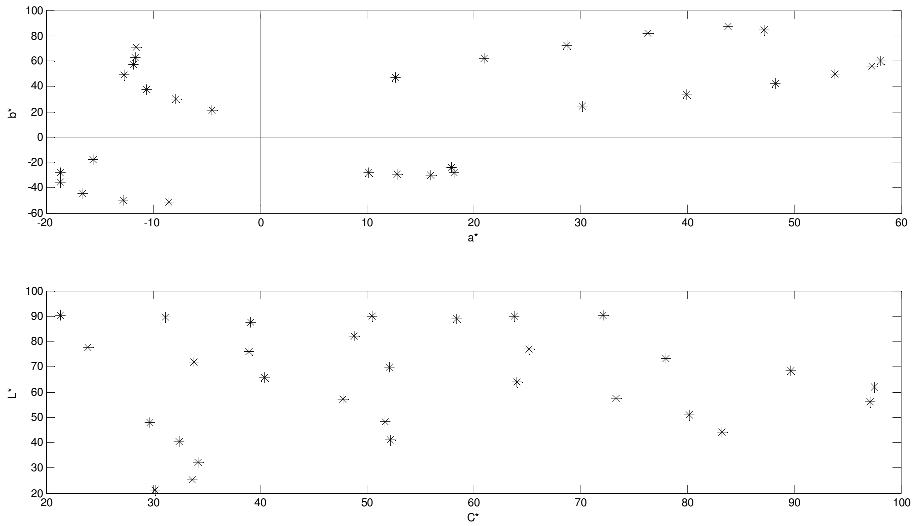

FIGURE 5: The CIE *a*b** and *C*L** Scatter Plots of 30 Colored Fabrics.

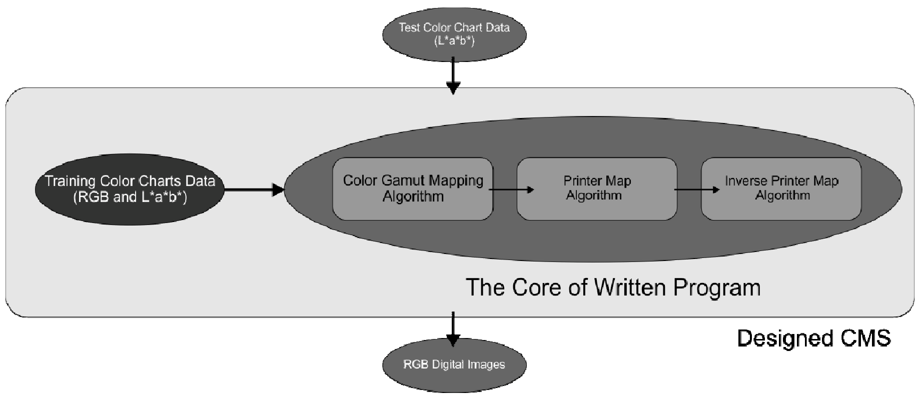

FIGURE 6: The Block Diagram of Designed CMS.

3.3. Evaluation of Color Management System

The performance of designed color management system was evaluated by calculating the CIELAB color difference values between the mapped initial CIELAB textile samples as the target colors (mapped $L^*a^*b^*$ in Figure 7) and the measured CIELAB values of color patches printed on the paper as the test chart (measured $L^*a^*b^*$ in Figure 7) using D65 standard illuminant and 1964 standard observer. While ICI algorithm was used for producing output RGB values, the calculated $L^*a^*b^*$ was the resultant of these RGB values. Hence the calculated ΔE^*_{ab} is the CIELAB color difference value between the mapped $L^*a^*b^*$ and the calculated $L^*a^*b^*$ values. In the case of calculated $L^*a^*b^*$ values tend to the mapped $L^*a^*b^*$, then the color difference between the mapped $L^*a^*b^*$ and the measured $L^*a^*b^*$ values becomes smaller. Figure 7 shows the workflow of the evaluation process.

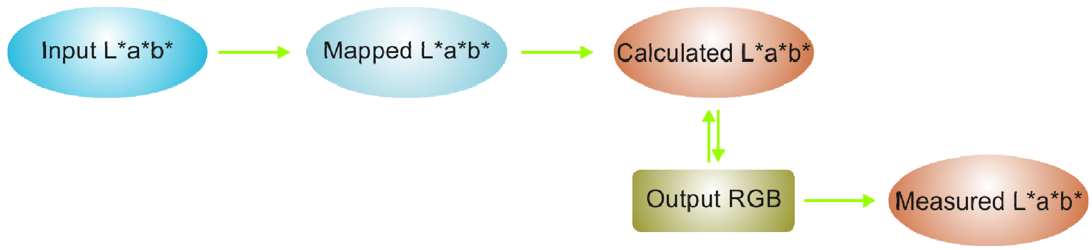

FIGURE 7: The Workflow for the Evaluation of Designed CMS.

4. RESULTS AND DISCUSSIONS

To evaluate the designed CMS, the colors of 30 colored fabrics were reproduced by the employed printer on the paper using the assembled color management system and the color difference values between the pairs were computed. The suggested recipes by the system were then employed for practical reproduction of colorimetric matches of colored fabrics on the paper and the color difference values were also measured. Since the printer inks were different from the textile dyestuffs, some colored fabrics were out of gamut and could not be reproduced by the printer primaries. Figure 8 shows the color gamut of the printer as well as the color specifications of targets, i.e. colored fabrics, in 3D space. It is evident in Figure 8 that some samples are out of printer gamut, hence the color gamut mapping process was performed before estimating the output RGB by intended CMS. So, the designed CMS model provided the mapped samples of those out of gamut colors before printing such samples on paper.

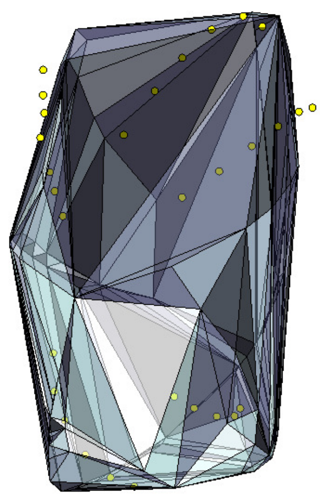

FIGURE 8: Color coordinates of the target fabrics (yellow dot points) with respect to the printer color gamut.

The average of the computed color differences between the targets and the estimated samples by the model as well as those between the targets and the physically printed samples are presented in Table 1. The table also shows the minimum, maximum, mean, median and the standard deviation of the color difference values. The reported results in Table 1 were achieved by creating the CMS with all 3164 available samples as the training chart. As the results shows, the median of the measured color differences is equal to 4.55 while, the minimum of 1.25 indicates to somehow large color difference value. The problem originates from the fact that the spectrophotometric and colorimetric properties of employed inks in printers were far from those dyestuffs that were employed in the textile industry. Furthermore, two different instruments with different geometries were employed for spectral and colorimetric measurement of papers and fabrics due to different surface properties. Besides, the reproducibility of the employed commercial printer was not high enough that could lead to some types of reproducibility problem.

Type of calculation	ΔE^*_{ab}				
	Min	**Max**	**Mean**	**Median**	**Std***
Calculated	0.85	10.14	4.55	4.48	2.48
Measured	1.25	10.45	4.70	4.55	2.29

* Standard Deviation

TABLE 1: The minimum, maximum, mean, median and standard deviation of the calculated and the measured color difference values between the colored fabrics and the reproduced samples on the paper under D65 and CIE 1964 standard observer.

Figure 9 shows the reflectance spectra of the six randomly selected targets and the corresponding matches on paper. Table 2 also shows the color differences values of these targets and the corresponding matches under D65, D50 and A standard illuminants. According to this table, different spectral behaviors of employed primaries in printers and dyes in the textiles have led to metameric (parameric) match that are more evident for samples #3, 5 and 6 by greater color difference values under different illuminants.

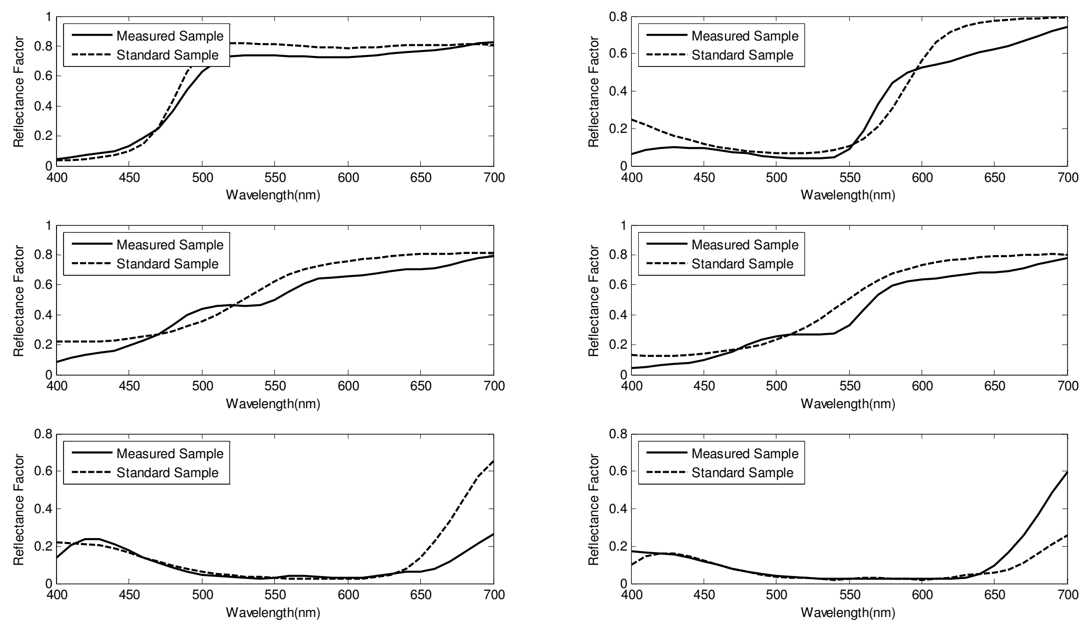

FIGURE 9: The reflectance spectra of 6 randomly selected targets and their corresponding matches.

Sample #	Illuminant		
	D65	D50	A
	ΔE^*_{ab}		
1	10.07	7.74	4.32
2	11.32	8.96	6.94
3	4.46	6.75	6.94
4	6.27	6.24	7.13
5	3.74	2.81	5.06
6	1.29	2.09	6.43

TABLE 2: The measured CIE ΔE^*_{ab} color difference values of 6 arbitrary selected colored targets and the corresponding matches under D65, D50 and A illuminants.

The effect of the number of training samples on the achieved color difference values was also studied. In fact, when the training samples are sparse, the chance of finding of samples in the region of target color would decrease. In order to investigate the effect of the number and the suitability of training samples on the performances of model, the reproducing procedure was carried out by using three different training sets. It is interesting that while the regression technique strongly depends on the specification of all samples in the training dataset, the interpolation technique based on LUT works locally and is only affected by the specifications of neighborhood samples around the desired sample. In fact, increasing the number of samples in training charts decreases the size of tessellation. So adding some extra samples in LUT could probably have no effect on the majority of other areas and therefore, on the final result. The examples of this issue are shown in Table 3 by reporting the color difference values of 10 randomly selected samples. The highlighted cells in the table show the color difference values that have not been affected by increasing the number of samples in the training charts. As mentioned earlier, increasing the color samples in the training chart at a given area does not guarantee the better performances for those in other areas. Figure 10 shows the scatter plot of a^* versus b^* values of color patches used in training sequence. As the figure shows, different numbers of training samples were used in LUT. The a^*b^* positions of the selected arbitrary samples are also shown by red circles in the plots. As Figure 10 demonstrates, the blank spaces in the LUT decreased by increasing of samples in training charts that could lead to more reliable results by improving the precision of the interpolation method. Thus, the appropriate learning based color reproduction system with acceptable results can be constructed by suitable as well as sufficient samples in the training charts whose color coordinates are properly distributed over the space.

Sample #	Sample specifications in CIE$L^*a^*b^*$ color system	ΔE^*_{ab} Number of samples in the training set		
		1400	2408	3164
1	$L^*=50, a^*=80, b^*=40$	10.64	3.55	3.55
2	$L^*=50, a^*=-80, b^*=40$	7.90	7.90	4.12
3	$L^*=50, a^*=80, b^*=-40$	10.75	4.41	4.41
4	$L^*=50, a^*=-80, b^*=-40$	4.81	4.81	4.81
5	$L^*=80, a^*=50, b^*=-20$	5.22	3.40	3.40
6	$L^*=20, a^*=-40, b^*=60$	6.54	6.54	5.62
7	$L^*=60, a^*=20, b^*=80$	14.75	7.17	5.19
8	$L^*=60, a^*=40, b^*=80$	22.84	6.60	6.60
9	$L^*=60, a^*=-20, b^*=-80$	15.35	15.35	8.58
10	$L^*=60, a^*=-20, b^*=80$	6.21	6.21	4.88

TABLE 3: The calculated color difference values against the number of samples in the training set.

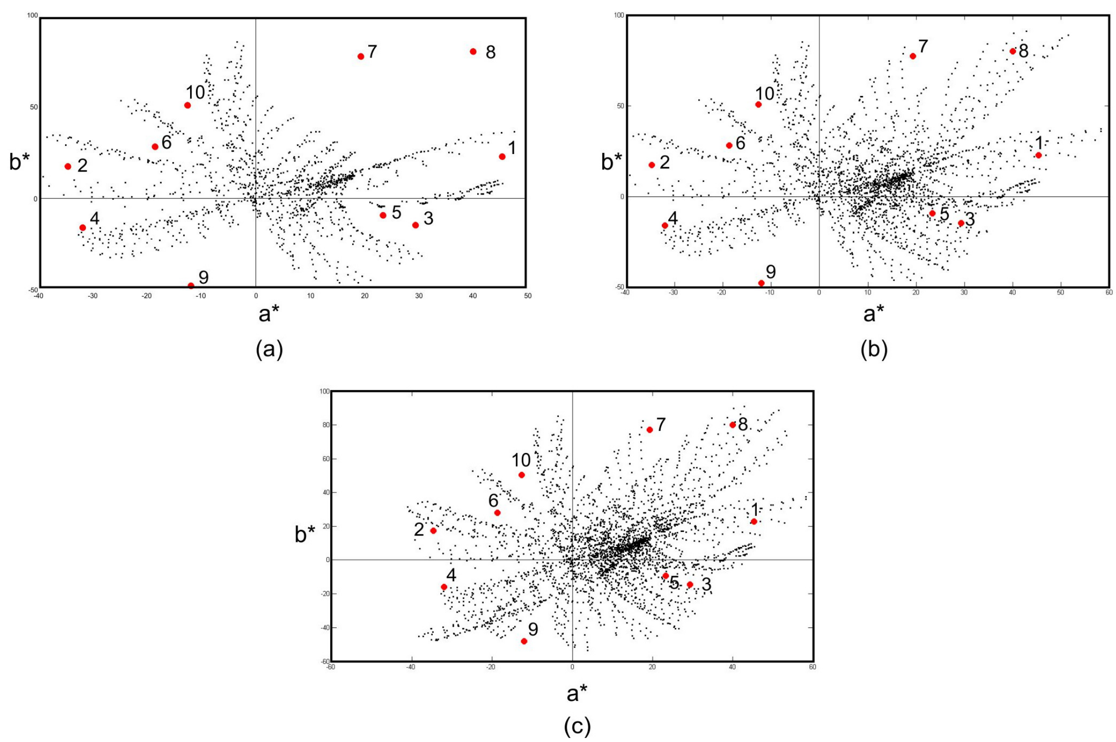

FIGURE 10: The CIE *a*b** scatter plot of color patches of the training charts. a) 1400 training samples, b) 2408 training samples and c) 3164 training samples. The red dots are the CIE a^*b^* specifications of 10 samples that their colors differences are reported in Table 3.

5. CONCLUSION

Implementing of an open loop color management system was suggested for colorimetric reproduction of a set of colored fabrics. To fulfill such plan, a color management system was designed to convert the CIELAB colorimetric coordinates to RGB values. By this arrangement, the system converted the analog CIE $L^*a^*b^*$ values of samples to digital RGB signals of printer.

The purpose was practically tested by designing a 3-D LUT technique to map between the color spaces. A set of color charts including of 3164 color patches was prepared to characterize the printer.

The designed color management system was assessed by colorimetric reproduction of a set of 30 colored fabrics on paper by a low price conventional printer. The CIELAB color coordinates of fabrics were introduced as inputs to a color management system and their colors were reproduced on desired paper using a characterized commercial inkjet printer. Then, the performance of the employed color reproduction system was practically examined by evaluating the color difference values between the targets and the corresponding matches reproduced on paper. The results of color reproduction were generally acceptable; nevertheless some samples suffered from somewhat high color difference values. It was shown that the accuracy of the system strongly depends on the number of samples in the training set together with their distribution in the color space.

It is essential to note that because of the process non-linearity, using the tetrahedral interpolation instead of polynomial transformation is either conventional or necessary in digital paper printing. But in comparison with other prevalent textile digital color management researches, Using the tetrahedral interpolation, gamut mapping, making custom training charts and results investigation are the novelties of this research in textile scope.

For future research it is suitable to use a color appearance model instead of a color model. A color appearance model matches the appearance of color and is independent from viewing condition. So having these kinds of models, the color reproduction process will be completed.

Also the result can be extended to paint, plastic and cosmetic industries for color reproduction using digital media.

6. REFERENCES

[1] E. Allen. “Basic Equations Used in Computer Color Matching”. J Opt. Soc. Am., vol. 56, pp.1256-1259, 1966.

[2] E. Allen. “Basic Equations Used in Computer Color Matching II”. J Opt. Soc. Am., vol. 64, pp. 991-993, 1974.

[3] P.H. McGinnis. “Spectrophotometric Color Matching with the Least Squares Technique”. Col. Eng., vol. 5, pp. 22-27, 1967.

[4] R.S. Berns, “A generic approach to color modeling”. Color Res. Appl., vol. 22, pp. 318-325, 1997.

[5] D.R. Wyble and R.S. Berns. “A Critical Review of Spectral Models Applied to Binary Color Printing”. Color Res. Appl., vol. 25, pp. 4-19, 2000.

[6] R.S. Berns, Billymer and Saltzman's Principles of Color Technology, 3rd ed., New York: Wiley and Sons, 2000.

[7] Y. Zhang, V. Cheung, S. Westland and K.J. Beverley. “Colour Management of a Low-Cost Four Colour Ink-Jet Printing System on Textiles”. Color. Technol., vol. 125, pp. 29-35 ,2009.

[8] C.D.M. Bezerra, C.J. Hawkyard, H.M. Kulube and R.S. Reyner. “Colour Matching for Ink-Jet Prints on Paper”. Color Res. Appl., vol. 23, pp. 18-26, 1998.

[9] S. Zuffi, R. Schettini and G. Mauri. “Spectral-based Printer Modeling and Characterization”. J Electron. Imaging, vol. 14, pp. 023008, 2005.

[10] S. Zuffi, R. Schettini and G. Mauri. “Using Genetic Algorithms for Spectral-based Printer Characterization”. In Proceedings of the IS&T's Conference on Image Quality, 2003, pp. 268-275.

[11] M.J. Vrhel. “Approximation of Color Characterization MLUTS with Artificial Neural Networks”. In Proceedings of the IEEE International Conference on Image Processing, 2003, pp. 465-468.

[12] M.J. Vrhel and H.J. Trussell. “Color Printer Characterization in MATLAB”. In Proceedings of the IEEE International Conference on Image Processing, 2002, pp. 457-460.

[13] G. Sharma. Digital Color Imaging Handbook, Boca Raton FL: CRC Press, 2003.

[14] L.K. Mestha and S.A. Dianat. Control of Color Imaging Systems, Analysis and Design”, 1st Ed., New York: CRC Press, 2009.

[15] D. Viassolo and L.K. Mestha. “A practical algorithm for the inversion of an experimental input-output color map for color correction”. J Opt. Eng., vol. 42, pp. 625, 2003.

[16] K. Braun, R. Balasubramanian and R. Eschbach. “Development and evaluation of six gamut-mapping algorithms for pictorial images”. In Proceedings of the IS&T and SID's 7th Color Imaging Conference, 1999, pp. 144-148.

[17] “RGB Printer Profiles: Adobe Photoshop CS3/CS4, Need To Know: X-Rite Color Service”.Internet:http://xritephoto.com/documents/literature/en/RGBPrinterNTK_EN.pdf, 2011.